ORGANOMETALLICS
Article
Cite This: Organometallics XXXX, XXX, XXX−XXX
pubs.acs.org/Organometallics

Electronic Ligand Modifications on Cobalt Complexes and Their Application toward the Semi-Hydrogenation of Alkynes and Para-Hydrogenation of Alkenes

Safiyah R. Muhammad, Joseph W. Nugent, Kenan Tokmic, Lingyang Zhu, Jumanah Mahmoud, and Alison R. Fout*

School of Chemical Sciences, University of Illinois at Urbana−Champaign, 600 South Mathews Avenue, Urbana, Illinois 61801, United States

Supporting Information

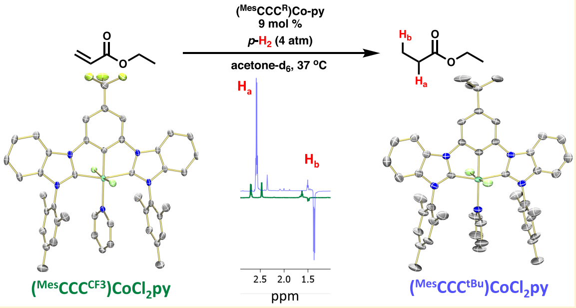

ABSTRACT: The effect of the electronic modification of a bis(carbene) pincer ligand, $(^{Mes}CCC^{R})$, on cobalt catalysis has been investigated. The pincer ligand was modified in the *para* position of the aryl backbone with a *tert*-butyl and trifluoromethyl moiety to yield the electronic variants that were applied toward the synthesis and characterization of several cobalt complexes, $(^{Mes}CCC^{R})Co$. The application of the $(^{Mes}CCC^{R})Co^{I}(N_2)PPh_3$ complexes toward the semihydrogenation of alkynes revealed that while the *tert*-butyl group does not impact reactivity, the loss of electron density at the metal center, by the installation of the CF_3 group, does affect product ratios. Further inspection of the proposed mechanism suggested that the installation of the trifluoromethyl group slows down olefin hydrogenation. This finding was further supported in the application of the $(^{Mes}CCC^{R})Co^{I}$-py (py = pyridine) complexes toward the *para*hydrogenation of ethyl acrylate, which demonstrated that the electron-withdrawing ligand variant produced less polarization.

INTRODUCTION

Modification of the steric and electronic properties of ligands to control the reactivity of metal centers is a common method employed by organometallic chemists to alter the catalytic properties of complexes.[1] Alteration of the electronic properties of ligands can largely effect the selectivity,[2−4] catalytic activity,[5,6] and mechanistic[7,8] pathways of these catalysts.

The chemistry of transition metals featuring meridional pincer ligands is an area that has benefited from the exploration of electronic modification to the ligand backbone. Small electronic and steric perturbations of these frameworks can have large effects on the reactivity of these systems. For example, studies done by the Chirik and Nakazawa groups have shown that electronic variation of their bis(imino)-pyridine iron complexes leads to the disruption of catalysis[9] or fluctuation of reaction rates, as dictated by the geometry imposed by such modifications.[10] Another example, offered by Brookhart and co-workers, showed that the electronic substitution in the *para* position of their bis(phosphonite) ligand influenced the initial turnover frequencies (TOF) of alkane transfer dehydrogenation.[11] They concluded that when there is less electron density at the metal center, the initial rates of the reaction are faster.

Chianese and co-workers developed and modified the ^{R}CCC (^{R}CCC = bis(aryl-benzimidazol-2-ylidene)phenyl)] pincer ligand used in this study. They reported the installation of a trifluoromethyl (CF_3) on their $(^{R}CCC)Ir$ complex and commented on its application in catalytic alkane dehydrogenation.[12] The analogous $(^{Mes}CCC)Co$, [^{Mes}CCC = bis(2,4,6-trimethylphenyl-benzimidazol-2-ylidene)phenyl)], system reported by our group has been previously employed for the catalytic hydrogenation of alkenes, alkynes, and nitriles.[13−15] In these studies, *para*hydrogen (p-H_2) was used as a spectroscopic tool to probe the mechanism of hydrogenation. The use of p-H_2 is a powerful tool in hydrogenation studies because it allows for signal amplification of hydrogenated products by NMR spectroscopy when certain conditions are met.[16] This allows for otherwise undetectable reaction intermediates to be observed under standard conditions. Observing the polarization of substrates allowed for the mechanism of alkene and alkyne hydrogenation to be proposed with the $(^{Mes}CCC)Co$ system.

Herein, we report the synthesis and characterization of both electron-rich and -poor analogues of $(^{Mes}CCC)Co$ complexes. Utilizing IR spectroscopy, the CO stretching frequencies were used to determine the perturbation of the electron density at the cobalt centers. These catalysts were then applied toward the semihydrogenation of alkynes and the *para*hydrogenation

Received: May 20, 2019

DOI: 10.1021/acs.organomet.9b00337

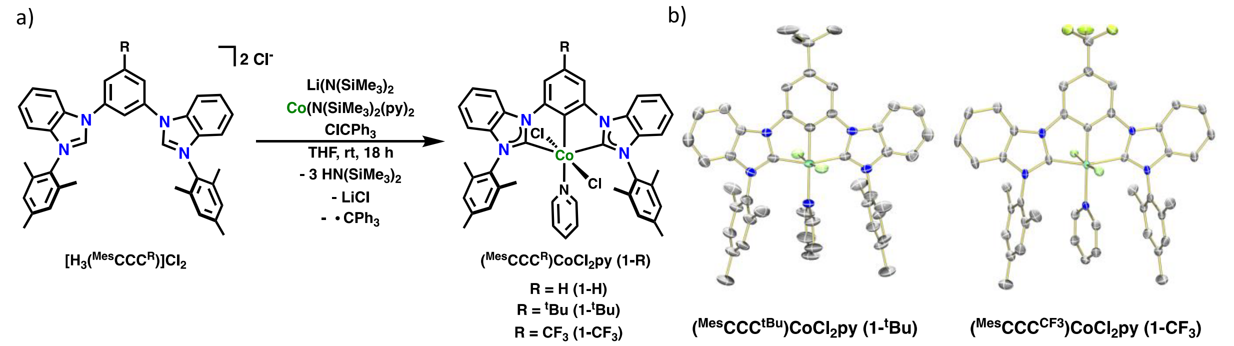

Figure 1. (a) Synthesis of complexes 1-R (R = H, ^{t}Bu, or CF_3). (b) X-ray crystal structures of 1-^{t}Bu and 1-CF_3 with the ellipsoids pictured at the 50% probability level (one out of two symmetrically independent molecules shown for 1-CF_3). Solvent molecules and hydrogen atoms have been omitted for clarity.

of ethyl acrylate, to investigate the effect of these perturbations on these catalytic processes.

RESULTS AND DISCUSSION

Synthesis of Modified Ligands. To achieve electronic modification without affecting the steric profile of the ligand framework, substituents were placed on the aryl ring in the position *para* to the C_{Ar}–Co bond formed upon metalation. The CF_3 group and *tert*-butyl (^{t}Bu) groups were chosen for their electronic properties and ease of ligand synthesis. The benzimidazolium salts, $[H_3({}^{Mes}CCC^{tBu})]Cl_2$ and $[H_3({}^{Mes}CCC^{CF3})]Cl_2$, were prepared following our modified literature procedure.[17,18]

Synthesis of $({}^{Mes}CCC^{R})CoCl_2py$ (1-R, R = ^{t}Bu and CF_3). Metalation of the benzimidazolium ligand salts, $[H_3({}^{Mes}CCC^{tBu})]Cl_2$ and $[H_3({}^{Mes}CCC^{CF3})]Cl_2$, following an established protocol[17] afforded the $({}^{Mes}CCC^{R})CoCl_2py$ products (R = ^{t}Bu (**1-^{t}Bu**) or CF_3 (**1-CF_3**)) as bright green powders in good yields (76% and 88%, respectively, Figure 1a). Characterization of **1-^{t}Bu** by ^{1}H NMR spectroscopy revealed a diamagnetic spectrum with 12 resonances, consistent with the formation of a low-spin, C_2-symmetric Co^{III} species, $({}^{Mes}CCC^{tBu})CoCl_2py$ complex (Figure S8).

Similarly, **1-CF_3** was characterized by ^{1}H NMR spectroscopy, with a diamagnetic spectrum containing 11 resonances and a ^{19}F NMR spectrum containing a single resonance at −61.04 ppm, consistent with the formation of $({}^{Mes}CCC^{CF3})CoCl_2py$ (Figures S10 and S12).

Crystals suitable for X-ray diffraction were grown from slow evaporation of a benzene (**1-^{t}Bu**) or chloroform (**1-CF_3**) solution at room temperature. Refinement of the structural data revealed the desired octahedral-Co^{III} complexes (Figure 1b and Table S3). The Co–C_{NHC} and Co–C_{Ar} bond lengths for **1-^{t}Bu** and **1-CF_3** were comparable to those of the previously reported $({}^{Mes}CCC)CoCl_2py$ complex, **1-H**,[17] as were the Co–N_{py} and Co–Cl distances for both complexes. In addition, the C_{Ar}–Co–N_{py} and C_{Ar}–Co–Cl bond angles of 179.63(12) and 85.80(10)/86.90(10)° for **1-^{t}Bu** and 179.51(22) and 85.56(17)/86.31(17)° for **1-CF_3** supported the predicted octahedral geometry. As expected, these results suggest that the electronic modification had no significant impact on the solid-state structure of the Co(III) complex.

Synthesis of Co(I) Complexes (2-R, 3-R, and 4-R). Given the stability of complexes **1-R** in air and water and the reactivity of previously isolated Co(I) complexes, we sought to synthesize the Co(I) analogues of **1-^{t}Bu** and **1-CF_3**. Treatment of **1-^{t}Bu** or **1-CF_3** with 2.5 equivalents of KC_8 resulted in the formation of a brown solution that, upon workup, yielded the $({}^{Mes}CCC^{R})$Co-py complexes (py = pyridine), **2-^{t}Bu** and **2-CF_3** (Figure 2). Characterization by ^{1}H and ^{13}C NMR spectroscopies confirmed the formation of new complexes, whose integrations were consistent with the pyridine-bound formulation (Figure S13–16). The ^{1}H NMR spectra display a broadening of the bound pyridine resonances and an overall shifting of the resonances upfield from the **1-R** complexes. The number of Mes-CH_3 resonances suggests that the **2-R** complexes retain their C_2-symmetry.

The stretching frequency of the carbonyl group by IR spectroscopy was shown by Tolman to reflect the strength of the other electron donor/acceptor ligands on the metal center.[19] Comparing the carbonyl stretching frequencies of the substituted complexes to the unmodified complex should provide data on the electronic influence of the ^{t}Bu or CF_3 ligand modification on the cobalt center. Therefore, the dicarbonyl species, $({}^{Mes}CCC^{R})Co(CO)_2$ (**3-H**, **3-^{t}Bu**, and **3-CF_3**) were synthesized in good yields from the reduction of complexes **1-H**, **1-^{t}Bu**, or **1-CF_3** with two equivalents of KC_8, followed by the addition of 1 atm of CO (Figure 2). Characterization by ^{1}H NMR spectroscopy revealed diamagnetic spectra, all consistent with the formation of a C_2-symmetric complex, with integration supporting the predicted $({}^{Mes}CCC^{R})Co(CO)_2$ formulation (Figures S17, S19, and S20). The ^{13}C NMR spectra of **3-R** were also consistent with this formulation, with the appearance of a new downfield resonance assigned to the ligated CO (Figures S18, S20, and S22).

Yellow crystals of **3-H**, suitable for single-crystal X-ray diffraction studies, were grown from a concentrated solution of THF. The crystal data revealed a five-coordinate cobalt complex with two carbonyl ligands on the metal center in a distorted trigonal bipyramidal geometry ($\tau = 0.55$),[20] as shown in Figure 2. The M–C_{aryl} bond is shorter than the length in analogous (POCOP)Co(I) dicarbonyl (POCOP = κ^3-C_6H_3-1,3-$[OPR_2]_2$, R = alkyl, aryl) pincer complexes reported by Heinekey,[21] and the (PCP)Fe(II) dicarbonyl (PCP = κ^3-C_6H_3-1,3-$[XPR_2]_2$, X = O, NH) complexes reported by Sortais and co-workers.[22] We attribute this, potentially, to the increased rigidity of the CCC ligand compared with the PCP ligands. The Co–C_{CO} bond length, 1.7776(19) Å, falls within the range of other reported Co(I) dicarbonyl complexes, 1.735(3)–1.800(1) Å.[23−27]

Characterization of **3-H** by infrared spectroscopy revealed two intense stretches at 1918 and 1973 cm^{-1} (Figure S23), corresponding to the two stretching modes expected for the dicarbonyl complex in a trigonal pyramidal geometry. The IR

DOI: 10.1021/acs.organomet.9b00337
Organometallics XXXX, XXX, XXX−XXX

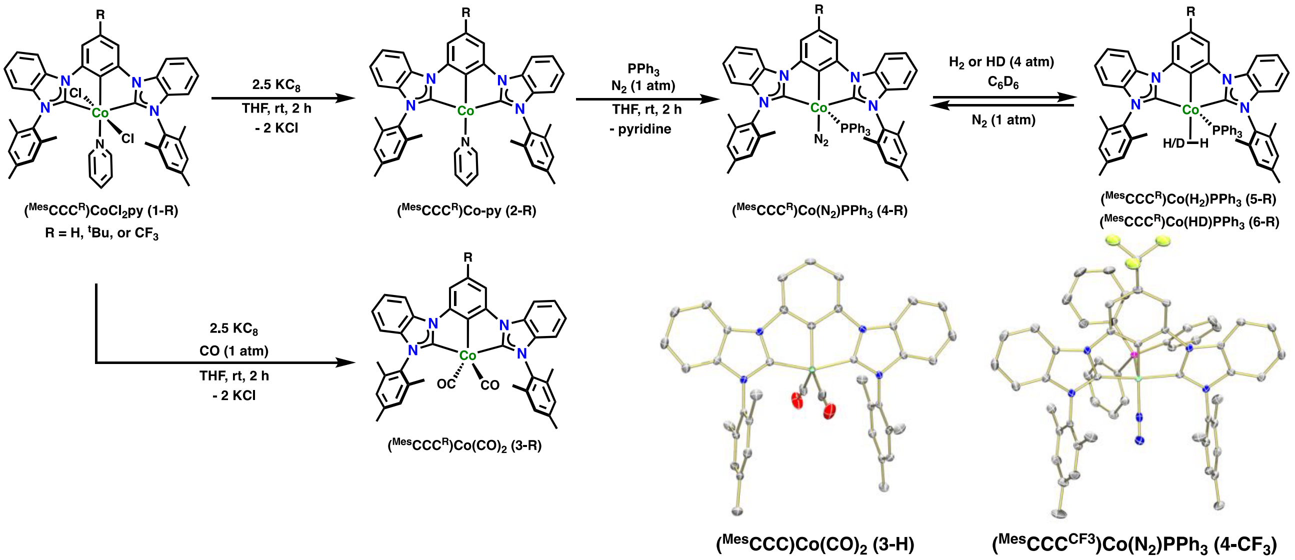

Figure 2. Synthesis of complexes 2-R, 3-R, 4-R, 5-R, and 6-R (R = H, ^{t}Bu, or CF_3). Crystal structures of 3-H and 4-CF_3 with the ellipsoids pictured at the 50% probability level. Solvent molecules and hydrogen atoms have been omitted for clarity.

spectra of **3-^{t}Bu** and **3-CF_3** also contained two stretches for the ligated CO (Figures S24 and S25), suggesting these complexes were isostructural to **3-H**. For **3-CF_3**, there is a blue shift in the C−O stretching frequencies, to 1951 and 2004 cm^{-1}, consistent with electron density being removed from the metal center. This suggests a weakening of the extent of π-backbonding which would strengthen the C−O bond in the carbonyl moieties. However, the values for **3-^{t}Bu** do not shift from **3-H** as expected, despite the presence of a more electron-donating R-group, as they also blue shift to 1939 and 1990 cm^{-1}. We hypothesize that because ^{t}Bu is a relatively weak electron donor, its effect may be more delocalized over the aryl backbone as opposed to that seen with the strongly electron-withdrawing CF_3 group.[28]

Previously, we reported the complex $(^{Mes}CCC)Co(N_2)PPh_3$ (**4-H**) (ν_{NN} = 2112 cm^{-1}) as a precatalyst for a variety of hydrogenation studies. We sought to isolate the analogous complexes with the modified ligands to then compare the reactivity of each. Addition of one equivalent of PPh_3 to **2-R** produced a red solution that upon workup yielded the corresponding $(^{Mes}CCC^{R})Co(N_2)PPh_3$ complexes, **4-R** (Figure 2). Characterization of **4-^{t}Bu** by ^{1}H NMR and ^{13}C NMR spectroscopies revealed spectra analogous to those reported for **4-H** (Figures S26 and S27).[17] Characterization by IR spectroscopy revealed a stretch at 2112 cm^{-1} that was assigned as the vibrational mode of a largely unactivated dinitrogen ligand (free dinitrogen ν_{NN} = 2331 cm^{-1})[29] and was consistent with the designation of this complex as $(^{Mes}CCC^{tBu})Co(N_2)PPh_3$ (Figure S31). Because of the lipophilicity of **4-^{t}Bu**, crystals suitable for X-ray diffraction were not able to be obtained.

Similarly, the ^{1}H and ^{13}C NMR spectra of **4-CF_3** is minorly perturbed from **4-H** and **4-^{t}Bu**, while the dinitrogen vibrational mode at 2123 cm^{-1} is consistent with the suggested formulation of $(^{Mes}CCC^{CF3})Co(N_2)PPh_3$ (Figures S28, S29, S32). The blue shift of the ligated N_2 in **4-CF_3** as compared with **4-H** and **4-^{t}Bu** further suggests that the installation of the electron-withdrawing group leads to less π back-donation into the dinitrogen antibonding orbitals, strengthening the N−N bond.

Crystallographic characterization of **4-CF_3** confirmed the expected distorted square pyramidal geometry at the cobalt center (τ = 0.14), with a bound dinitrogen ligand *trans* to the Co−C_{Ar} bond (Figure 2). We proposed that if there is indeed less π back-bonding, there would be a strengthening of the Co−C_{Ar} bond, while the Co−N bond would weaken in the structure of **4-CF_3** when compared to **4-H**. The Co−C_{Ar} bond was found to be 1.8677(21) Å, slightly shortened from the bond length of 1.8750(13) Å in **4-H**. The Co−N bond distance of 1.8412(19) Å is elongated from that of 1.8270(12) Å observed in **4-H**. The N−N bond distance of 1.0873(26) Å is consistent with a relatively unactivated N_2 ligand (free N_2 at 1.0975(1) Å).[30]

Reactivity of $(^{Mes}CCC^{R})Co(N_2)PPh_3$ (4-R) with H_2 and D_2. In our previous reports of the hydrogenation of olefins and alkynes, the active catalyst was proposed to be the cobalt(I)-dihydrogen complex, $(^{Mes}CCC)Co(H_2)PPh_3$ (**5-H**). Therefore, to understand how electronic modifications might affect the formation of the dihydrogen complex, we sought to synthesize this complex with the modified ligands. Exposure of a benzene-d_6 solution of **4-^{t}Bu** to 1 atm of H_2(g) at 77 K resulted in an immediate color change of the solution from red to orange (Figure 2). ^{1}H NMR spectroscopy revealed a diamagnetic spectrum with features distinct from the starting complex. A resonance at 4.47 ppm was assigned to free H_2(g) and a broad resonance at −5.39 ppm, integrating to 2H, was assigned as the bound H_2 molecule in the proposed $(^{Mes}CCC^{tBu})Co(H_2)PPh_3$ complex, **5-^{t}Bu** (Figure S33). Similar treatment of **4-CF_3** with H_2(g) yielded a ^{1}H NMR spectrum with a broad resonance located at −5.26 ppm, integrating for 2H, which too was assigned as bound dihydrogen (Figure S34). All other resonances were consistent with the formation of the $(^{Mes}CCC^{CF3})Co(H_2)PPh_3$ complex, **5-CF_3**. It was previously reported that exposure of **5-H** to a dinitrogen atmosphere resulted in the displacement of the bound H_2 by N_2 to regenerate **4-H**.[13] Similarly, when **5-^{t}Bu** and **5-CF_3** were re-exposed to a dinitrogen atmosphere, an immediate color change from orange to red was noted, indicating reformation of the dinitrogen complexes **4-^{t}Bu** and **4-CF_3** (confirmed by ^{1}H NMR spectroscopy).

To further test the effect of ligand modification on the lability of the H_2 ligand, we measured the exchange rate of bound H_2 with free H_2. A spin saturation study was conducted on each dihydrogen complex which revealed that the exchange rates for **4-H**, **^{t}Bu**, and **CF_3** were 0.25, 0.31, and 0.30, respectively, demonstrating that ligand substitution does not significantly impact H_2 lability.

Our group has shown previously that upon exposure of **4-H** to HD gas, the complex generates **6-H**, (^{Mes}CCC)Co(HD)-PPh_3, as well as H_2 and D_2(g). Similarly, upon exposure of **4-H** to a 50:50 mixture of H_2 and D_2(g), HD gas was generated (Figure 2).[13] Both experiments provide evidence that the dinitrogen complex activates H_2/D_2 to generate transient Co-hydrides/deuterides that reductively eliminate to form HD or H_2/D_2. Because of the modified electron density at the cobalt center, we sought to explore if the H_2 activation chemistry may have been altered.[31] To this end, complexes **4-^{t}Bu** and **4-CF_3** were treated with 1 atm of a 50:50 mixture of H_2 and D_2 gas at 77 K. The ^{1}H NMR spectra of the resulting complexes revealed the presence of free H_2 gas at 4.47 ppm, a triplet at 4.43 ppm which was assigned to free HD gas, and doublet of triplets at −5.46 and −5.42 ppm for (^{Mes}CCC^{tBu})Co(HD)-PPh_3, **6-^{t}Bu**, and −5.33 and −5.28 ppm for (^{Mes}CCC^{CF3})Co-(HD)PPh_3, **6-CF_3**, which were assigned to the bound HD molecule (Figures S35 and S36). The J_{HD} coupling constants for the bound HD triplets were 31 and 33 Hz for **6-^{t}Bu** and **6-CF_3**, respectively, both comparable to that of **6-H** at 33 Hz. Utilizing the correlations established by Morris,[32] we calculated the d_{HH} to be 0.90 and 0.87 Å for **6-^{t}Bu** and **6-CF_3**, respectively, which is consistent with other Co(I)-H_2 complexes.[33,34]

Alkyne Semi-Hydrogenation Studies. With evidence demonstrating similarities in the ability of the modified complexes to interact with dinitrogen and dihydrogen, their catalytic performance was evaluated to determine if electronic differences would impact their catalytic performance. Our group has previously reported the semihydrogenation of internal alkynes bearing various functionalities with **4-H**; therefore, this was chosen as a model reaction to benchmark the modified ligand frameworks in catalysis.[14] As depicted in Table 1, three substrates were compared and analyzed for product distribution and ratios of the E to Z isomers formed.

Studies were conducted using previously optimized conditions for catalyst **4-H** with 4 atm of H_2 gas at 30 °C in THF for 17 h. Diphenylacetylene showed complete conversion of the starting alkyne to a ratio of the E-alkene and alkane when **4-H** was the catalyst. Interestingly, while **4-^{t}Bu** performed on par with **4-H** in terms of the ratio of desired alkene to alkane, **4-CF_3** generated a significantly less amount of the alkane, 5% compared to the 18% from **4-H**. Similarly, for trimethyl(thiophen-3-ylethynyl)silane, **4-CF_3** outperformed both the original catalyst and **4-^{t}Bu**. This theme was consistent with ((2-bromophenyl)ethynyl)trimethylsilane, as well, with both **4-^{t}Bu** and **4-CF_3**, showing incomplete isomerization of the Z isomer to the E isomer.

Table 1. Alkyne Semihydrogenation Data with 4-R[a]

	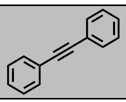	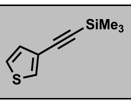	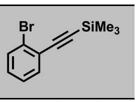
4-H	82% (18%) >99	64% (22%) >99	70% (30%) >99
4-^{t}Bu	84% (16%) >99	86% (13%) >99	86% (14%) 61:39
4-CF_3	95% (5%) >99	88% (12%) >99	97% (2%) 38:62

[a] The first value is the alkene yield, the value in parentheses is the alkane yield, and the third value below is the E:Z isomer ratio. Each is given as an average of duplicate runs.

To better understand whether the proposed mechanism[14] of *cis*-hydrogenation, followed by *trans*-isomerization was being affected by the installation of the CF_3 moiety, *para*hydrogen induced polarization (PHIP) transfer studies were used to track the addition of hydrogen onto the substrate (see pages S33−36). The addition of *para*-hydrogen (p-H_2) to unsaturated substrates allows for signal amplification of the hydrogenated product by NMR spectroscopy, making the detection of reaction intermediates, undetectable under standard conditions, accessible. In order to observe signal enhancement with p-H_2 some conditions must be met: the H atoms from a single p-H_2 molecule must be added in a pairwise fashion to the same substrate in magnetically distinct positions.[16,35] Utilizing a 45° pulse and a double quantum OPSY (Only *Para*hydrogen Spectroscopy) filter,[36] we were able to investigate trimethyl(thiophen-3-ylethynyl)silane under catalytic conditions (Figure 3). With **4-^{t}Bu** and **4-CF_3** as the catalysts, the only hyperpolarized intermediate observed was that of the *cis*-hydrogenated product, with a $^3J_{HH}$ coupling constants of 13.8 and 14.0 Hz for **4-^{t}Bu** and 14.3 and 14.3 Hz for **4-CF_3** (the *trans*-hydrogenated product has $^3J_{HH}$ coupling constants of 18.8 Hz).[37] This suggests that the reaction still proceeds through *cis*-hydrogenation followed by *trans*-isomerization to yield the products observed by GC-MS and NMR spectroscopy.

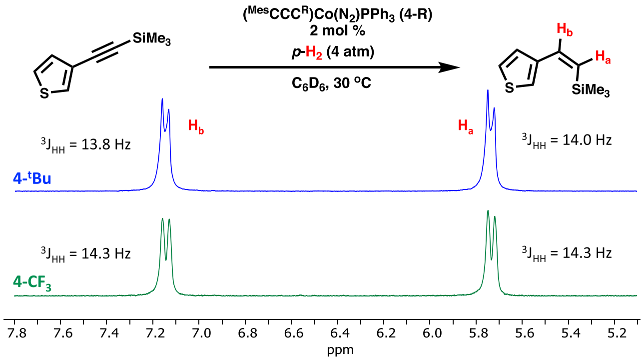

Figure 3. *Para*hydrogenation of trimethyl(thiophen-3-ylethynyl)silane to the cis-isomer by 4-^{t}Bu and 4-CF_3.

We propose that the modification of the electronic properties of the catalyst does not interfere with the proposed mechanism (*cis*-hydrogenation followed by *trans*-isomerization) (Figure S56); however, the installation of the electron withdrawing group does influence alkene hydrogenation, as a decreased production of the overhydrogenated product (alkane) was observed. With the use of **4-CF_3**, olefin activation may be the new rate-determining step since neither the binding of alkyne nor its activation is being hindered on the same time scale (alkynes were completely hydrogenated). In addition, H_2/D_2 exchange experiments and calculated bond lengths of H_2 support that the activation of H_2 is not affected and therefore not responsible for the differing product ratios.

In order to probe olefin activation, **4-R** was reacted with 4-vinylcyclohexene and H_2(g) and the reaction was monitored by ^1H NMR spectroscopy (Figures S47 and S48). Catalyst **4-H** converts 4-vinylcyclohexene to 4-ethylcyclohexene in 2 h, while at the same time point, only 52% of the 4-ethylcyclohexene product is formed when **4-CF_3** is used as the catalyst. This result supports that alkene hydrogenation is impacted by the ligand modification in **4-CF_3**.

***Para*hydrogenation of Ethyl Acrylate.** Lastly, we wanted to study how the installation of these modifying groups would effect the signal enhancement observed with the use of *para*-hydrogen. Recently, we have shown the use of **2-H** as a PHIP catalyst in the hydrogenation of ethyl acrylate to ethyl propionate.[38] The hyperpolarization of ethyl propionate in the ^1H spectrum was observed, and the transfer of polarization to neighboring ^{13}C nuclei, notably to the carbonyl moiety, was observed in the ^{13}C spectrum. Given the differences observed in the alkyne and alkene hydrogenation studies, especially for **4-CF_3**, we were curious how the ligand modification would impact the overall polarization of ethyl propionate.

For direct comparisons, the catalytic conditions reported for **2-H** were used in this study. The catalyst (**2-^{t}Bu** or **2-CF_3** at 9% loading) was reacted with ethyl acrylate and 4 atm of p-H_2 to produce ethyl propionate. The reaction was studied by ^1H and ^{13}C NMR spectroscopies at low magnetic field (~0.5 gauss). As depicted in Figure 4, both **2-^{t}Bu** and **2-CF_3** were capable of hyperpolarizing the ethyl propionate product, with the ^1H NMR spectra showing the emissive and absorptive resonances expected for a reaction taking place at a low magnetic field (Figure 4, see SI for more information).[39]

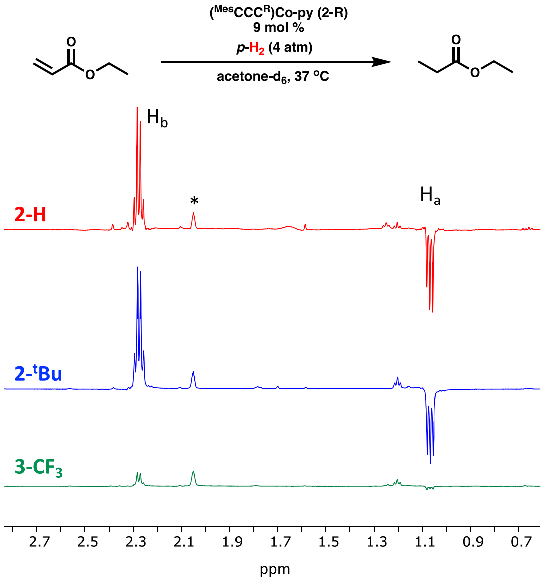

Figure 4. *Para*hydrogenation of ethyl acrylate by 2-R, ^1H NMR spectra.

The extent of polarization in the ^1H NMR spectrum for **2-^{t}Bu** was comparable to that of **2-H**; however, the polarization by **2-CF_3** was significantly reduced in comparison. This is consistent with the trifluoromethyl installation resulting in a slower olefin hydrogenation. Since there was not a significant concentration of hydrogenated product due to slow olefin hydrogenation, there was no buildup of polarization (see SI for requirements for observance of polarization).

Although the spontaneous transfer of polarization is not thought to be dependent on the catalyst, but only on the magnetic field, the presence of catalyst can increase relaxation of the polarized product, thus decreasing the height of the polarized signal. Monitoring the catalysis by ^{13}C spectroscopy revealed that both **2-^{t}Bu** and **2-CF_3** are able to catalyze the polarization of α, β, and carbonyl carbons, albeit with lower signal enhancement than that observed with **2-H** (Figures S52 and S54).

■ CONCLUSIONS

In conclusion, a series of cobalt complexes bearing the electronically modified monoanionic bis(carbene) ($^{Mes}CCC^R$) ligand, with a trifluoromethyl group as the electron-withdrawing moiety and the *tert*-butyl group for the electron-donating moiety were synthesized. The dicarbonyl complexes were synthesized to quantify the electron density at cobalt by IR spectroscopy, revealing a blue shift in the C−O frequencies for the CF_3 functionalized ligand, consistent with less π-backbonding. The *tert*-butyl group is thought to impart a weak effect on the cobalt center, which unexpectedly also leads to a slight blue shift in the carbonyl stretching frequencies.

The $Co^I(H_2)$ complexes, **5-^{t}Bu** and **5-CF_3**, demonstrated H_2 activation chemistry analogous to the unmodified complex, leading us to examine complexes **4-^{t}Bu** and **4-CF_3** as catalysts in the semihydrogenation of internal alkynes. Results showed that **4-^{t}Bu** performs comparably to the unmodified (^{Mes}CCC)-$Co(N_2)PPh_3$ complex; however, **4-CF_3** resulted in less overhydrogenation of the alkene, suggesting that it may be a slower catalyst. Closer examination of the olefin hydrogenation process revealed that the activation of olefin is hampered by the installation of the CF_3 group, explaining the lower amounts of alkane product observed. Application of the ($^{Mes}CCC^R$)Co-py complexes, **2-^{t}Bu** and **2-CF_3**, toward the *para*hydrogenation of ethyl acrylate demonstrated their ability to facilitate signal enhancement and polarization transfer to neighboring nuclei, albeit at lower yields for **2-CF_3**. Overall, the *tert*-butyl functionalization had little effect on the reactivity of the resulting Co complexes; however, the electron-withdrawing trifluoromethyl group altered the selectivity of the semi-hydrogenation of alkynes. This altered selectivity stems from the diminished reactivity toward alkene hydrogenation, which was suggested by the hydrogenation of 4-vinylhexene and corroborated by *para*hydrogenation of ethyl acrylate.

■ ASSOCIATED CONTENT

Ⓢ Supporting Information

The Supporting Information is available free of charge on the ACS Publications website at DOI: 10.1021/acs.organomet.9b00337.

Experimental data (PDF)

Accession Codes

CCDC 1917121−1917124 contain the supplementary crystallographic data for this paper. These data can be obtained free of charge via www.ccdc.cam.ac.uk/data_request/cif, or by emailing data_request@ccdc.cam.ac.uk, or by contacting The Cambridge Crystallographic Data Centre, 12 Union Road, Cambridge CB2 1EZ, UK; fax: +44 1223 336033.

■ AUTHOR INFORMATION

Corresponding Author

*E-mail for A.R.F.: fout@illinois.edu.

ORCID

Alison R. Fout: 0000-0002-4669-5835

Notes

The authors declare no competing financial interest.

■ ACKNOWLEDGMENTS

The authors thank the NSF for financial support with a CAREER award (1351961) to ARF. SRM thanks the Ford Foundation for a predoctoral graduate fellowship. Lastly, the authors also thank Dr. Toby Woods and Dr. Danielle Gray for assistance with crystallography.

■ REFERENCES

(1) Peris, E.; Crabtree, R. H. Key Factors in Pincer Ligand Design. *Chem. Soc. Rev.* **2018**, *47*, 1959−1968.

(2) Hyster, T. K.; Rovis, T. Pyridine Synthesis from Oximes and Alkynes via Rhodium(III) Catalysis: Cp* and Cp^t Provide Complementary Selectivity. *Chem. Commun.* **2011**, *47*, 11846−11848.

(3) Popeney, C.; Guan, Z. Ligand Electronic Effects on Late Transition Metal Polymerization Catalysts. *Organometallics* **2005**, *24*, 1145−1155.

(4) Biberger, T.; Gordon, C. P.; Leutzsch, M.; Peil, S.; Guthertz, A.; Copéret, C.; Fürstner, A. Alkyne Gem-Hydrogenation: Formation of Pianostool Ruthenium Carbene Complexes and Analysis of Their Chemical Character. *Angew. Chemie - Int. Ed.* **2019**, *58*, 1−7.

(5) Sandhya, K. S.; Remya, G. S.; Suresh, C. H. Pincer Ligand Modifications to Tune the Activation Barrier for H_2 Elimination in Water Splitting Milstein Catalyst. *Inorg. Chem.* **2015**, *54*, 11150−11156.

(6) Li, H.; Gonçalves, T. P.; Lupp, D.; Huang, K.-W. PN^3(P)-Pincer Complexes: Cooperative Catalysis and Beyond. *ACS Catal.* **2019**, *9*, 1619−1629.

(7) Virca, C. N.; Lohmolder, J. R.; Tsang, J. B.; Davis, M. M.; McCormick, T. M. Effect of Ligand Modification on the Mechanism of Electrocatalytic Hydrogen Production by Ni(Pyridinethiolate)$_3^-$ Derivatives. *J. Phys. Chem. A* **2018**, *122*, 3057−3065.

(8) Gies, A. P.; Kuhlman, R. L.; Zuccaccia, C.; MacChioni, A.; Keaton, R. J. Mass Spectrometric Mechanistic Investigation of Ligand Modification in Hafnocene-Catalyzed Olefin Polymerization. *Organometallics* **2017**, *36*, 3443−3455.

(9) Archer, A. M.; Bouwkamp, M. W.; Cortez, M.-P.; Lobkovsky, E.; Chirik, P. J. Arene Coordination in Bis(Imino)Pyridine Iron Complexes: Identification of Catalyst Deactivation Pathways in Iron-Catalyzed Hydrogenation and Hydrosilation. *Organometallics* **2006**, *25*, 4269−4278.

(10) Toya, Y.; Hayasaka, K.; Nakazawa, H. Hydrosilylation of Olefins Catalyzed by Iron Complexes Bearing Ketimine-Type Iminobipyridine Ligands. *Organometallics* **2017**, *36*, 1727−1735.

(11) Göttker-Schnetmann, I.; White, P.; Brookhart, M. Iridium Bis(Phosphinite) p-XPCP Pincer Complexes: Highly Active Catalysts for the Transfer Dehydrogenation of Alkanes. *J. Am. Chem. Soc.* **2004**, *126*, 1804−1811.

(12) Chianese, A. R.; Drance, M. J.; Jensen, K. H.; McCollom, S. P.; Yusufova, N.; Shaner, S. E.; Shopov, D. Y.; Tendler, J. A. Acceptorless Alkane Dehydrogenation Catalyzed by Iridium CCC-Pincer Complexes. *Organometallics* **2014**, *33*, 457−464.

(13) Tokmic, K.; Markus, C. R.; Zhu, L.; Fout, A. R. Well-Defined Cobalt(I) Dihydrogen Catalyst: Experimental Evidence for a Co(I)/Co(III) Redox Process in Olefin Hydrogenation. *J. Am. Chem. Soc.* **2016**, *138*, 11907−11913.

(14) Tokmic, K.; Fout, A. R. Alkyne Semihydrogenation with a Well-Defined Nonclassical Co-H_2 Catalyst: A H_2 Spin on Isomerization and E-Selectivity. *J. Am. Chem. Soc.* **2016**, *138*, 13700−13705.

(15) Tokmic, K.; Jackson, B. J.; Salazar, A.; Woods, T. J.; Fout, A. R. Cobalt-Catalyzed and Lewis Acid-Assisted Nitrile Hydrogenation to Primary Amines: A Combined Effort. *J. Am. Chem. Soc.* **2017**, *139*, 13554−13561.

(16) Duckett, S. B.; Mewis, R. E. Application of Para Hydrogen Induced Polarization Techniques in NMR Spectroscopy and Imaging. *Acc. Chem. Res.* **2012**, *45*, 1247−1257.

(17) Ibrahim, A. D.; Tokmic, K.; Brennan, M. R.; Kim, D.; Matson, E. M.; Nilges, M. J.; Bertke, J. A.; Fout, A. R. Monoanionic Bis(Carbene) Pincer Complexes Featuring Cobalt(I-III) Oxidation States. *Dalt. Trans.* **2016**, *45*, 9805−9811.

(18) Martinez, G. E.; Nugent, J. W.; Fout, A. R. Simple Nickel Salts for the Amination of (Hetero)Aryl Bromides and Iodides with Lithium Bis(Trimethylsilyl)Amide. *Organometallics* **2018**, *37*, 2941−2944.

(19) Tolman, C. A. Steric Effects of Phosphorus Ligands in Organometallic Chemistry and Homogeneous Catalysis. *Chem. Rev.* **1977**, *77*, 313−348.

(20) Addison, A. W.; Rao, T. N.; Reedijk, J.; van Rijn, J.; Verschoor, G. C. Synthesis, Structure, and Spectroscopic Properties of Copper(II) Compounds Containing Nitrogen-Sulphur Donor Ligands; the Crystal and Molecular Structure of Aqua[1,7-Bis(N-Methylbenzimidazol-2′-Yl)- 2,6-Dithiaheptane]Copper(II) Perchlorate. *J. Chem. Soc., Dalton Trans.* **1984**, 1349−1356.

(21) Guard, L. M.; Hebden, T. J.; Linn, D. E., Jr.; Heinekey, D. M. Pincer-Supported Carbonyl Complexes of Cobalt(I). *Organometallics* **2017**, *36*, 3104−3109.

(22) Jiang, S.; Quintero-Duque, S.; Roisnel, T.; Dorcet, V.; Grellier, M.; Sabo-Etienne, S.; Darcel, C.; Sortais, J.-B. Direct Synthesis of Dicarbonyl PCP-Iron Hydride Complexes and Catalytic Dehydrogenative Borylation of Styrene. *Dalt. Trans.* **2016**, *45*, 11101−11108.

(23) Zhang, H.; Xing, J.; Dong, Y.; Xie, S.; Ren, S.; Qi, X.; Sun, H.; Li, X.; Fuhr, O.; Fenske, D. Phosphine-Assisted C − H Bond Activation in Schiff Bases and Formation of Novel Organo Cobalt Complexes Bearing Schiff Base Ligands. *New J. Chem.* **2018**, *42*, 4646−4652.

(24) Mills, M. R.; Barnes, C. L.; Bernskoetter, W. H. Influences of Bifunctional PNP-Pincer Ligands on Low Valent Cobalt Complexes Relevant to CO_2 Hydrogenation. *Inorg. Chem.* **2018**, *57*, 1590−1597.

(25) Yuan, S.; Sun, H.; Zhang, S.; Li, X. Synthesis of Fluorophenyl Carbonyl Cobalt(I) Complexes and Decarbonylation of 2,4,5-Trifluorobenzaldehyde Catalyzed by CoMe(PMe$_3$)$_4$. *Inorg. Chim. Acta* **2016**, *439*, 100−105.

(26) Spentzos, A. Z.; Barnes, C. L.; Bernskoetter, W. H. Effective Pincer Cobalt Precatalysts for Lewis Acid Assisted CO_2 Hydrogenation. *Inorg. Chem.* **2016**, *55*, 8225−8233.

(27) Krafft, M. J.; Bubrin, M.; Paretzki, A.; Lissner, F.; Fiedler, J.; Zálîs, S.; Kaim, W. Identifying Intermediates of Sequential Electron and Hydrogen Loss from a Dicarbonylcobalt Hydride Complex. *Angew. Chem., Int. Ed.* **2013**, *52*, 6781−6784.

(28) Hansch, C.; Leo, A.; Taft, R. W. A Survey of Hammett Substituent Constants and Resonance and Field Parameters. *Chem. Rev.* **1991**, *91*, 165−195.

(29) Dugan, T. R.; Macleod, K. C.; Brennessel, W. W.; Holland, P. L. Cobalt−Magnesium and Iron−Magnesium Complexes with Weakened Dinitrogen Bridges. *Eur. J. Inorg. Chem.* **2013**, *2013*, 3891−3897.

(30) Huber, K. P.; Herzberg, G. Constants of diatomic molecules.*Molecular Spectra and Molecular Structure*; Springer: Boston, MA, 1979; pp 8−689.

(31) Rozenel, S. S.; Padilla, R.; Camp, C.; Arnold, J. Unusual Activation of H_2 by Reduced Cobalt Complexes Supported by a PNP Pincer Ligand. *Chem. Commun.* **2014**, *50*, 2612−2614.

(32) Maltby, P. A.; Schlaf, M.; Steinbeck, M.; Lough, A. J.; Morris, R. H.; Klooster, W. T.; Koetzle, T. F.; Srivastava, R. C. Dihydrogen with Frequency of Motion Near the 1H Larmor Frequency. Solid-State Structures and Solution NMR Spectroscopy of Osmium Complexes Trans -[Os(H··H)X(PPh$_2$CH$_2$CH$_2$PPh$_2$)$_2$]$^+$. *J. Am. Chem. Soc.* **1996**, *118*, 5396−5407.

(33) Hebden, T. J.; St. John, A. J.; Gusev, D. G.; Kaminsky, W.; Goldberg, K. I.; Heinekey, D. M. Preparation of a Dihydrogen Complex of Cobalt. *Angew. Chem.* **2011**, *123*, 1913−1916.

(34) Suess, D. L. M.; Tsay, C.; Peters, J. C. Dihydrogen Binding to Isostructural S = 1/2 and S═0 Cobalt Complexes. *J. Am. Chem. Soc.* **2012**, *134*, 14158−14164.

(35) Cavallari, E.; Carrera, C.; Reineri, F. ParaHydrogen Hyperpolarized Substrates for Molecular Imaging Studies. *Isr. J. Chem.* **2017**, *57*, 833−884.

(36) Aguilar, J. A.; Adams, R. W.; Duckett, S. B.; Green, G. G. R.; Kandiah, R. Selective Detection of Hyperpolarized NMR Signals Derived from Para-Hydrogen Using the Only Para-Hydrogen SpectroscopY (OPSY) Approach. *J. Magn. Reson.* **2011**, *208*, 49−57.

(37) Karabelas, K.; Hallberg, A. Synthesis of (E)-(2-Arylethenyl)-Silanes by Palladium-Catalyzed Arylation of Vinylsilanes in the Presence of Silver Nitrate. *J. Org. Chem.* **1986**, *51*, 5286−5290.

(38) Tokmic, K.; Greer, R. B.; Zhu, L.; Fout, A. R. ^{13}C NMR Signal Enhancement Using Parahydrogen-Induced Polarization Mediated by a Cobalt Hydrogenation Catalyst. *J. Am. Chem. Soc.* **2018**, *140*, 14844−14850.

(39) Pravica, M. G.; Weitekamp, D. P. Net NMR Alignment by Adiabatic Transport of Parahydrogen Addition Products to High Magnetic Field. *Chem. Phys. Lett.* **1988**, *145*, 255−258.

DOI: 10.1021/acs.organomet.9b00337